Eur. Phys. J. C 52, 625–633 (2007)
DOI 10.1140/epjc/s10052-007-0411-7

THE EUROPEAN PHYSICAL JOURNAL C

Regular Article – Theoretical Physics

Higgs and Z' phenomenology in $B-L$ extension of the standard model at LHC

W. Emam[1,2], S. Khalil[1,2,a]

[1] Center for Theoretical Physics at the British University in Egypt, Sherouk City, Cairo 11837, Egypt
[2] Faculty of Science, Ain Shams University, Cairo 11566, Egypt

Received: 17 May 2007 / Revised version: 31 July 2007 /
Published online: 2 October 2007 –

Abstract. The phenomenology of the low scale $\mathrm{U}(1)_{B-L}$ extension of the standard model and its implications at LHC energies is presented. In this model, an extra gauge boson corresponding to B–L gauge symmetry and an extra SM singlet scalar (heavy Higgs boson) are predicted. We show a detailed analysis of both heavy and light Higgs bosons decay and production in addition to the possible decay channels of the new gauge boson. We find that the cross sections of the SM-like Higgs production are reduced by $\sim 20\%$–30%, while its decay branching ratios remain intact. The extra Higgs boson has relatively small cross sections and the branching ratios of $Z' \to l^+l^-$ are of order $\sim 20\%$ to be compared to $\sim 3\%$ of the SM results. Hence, the search for Z' is accessible via a clean dilepton signal at LHC.

1 Introduction

The standard model (SM) of elementary particles has been regarded only as a low energy effective theory of the yet-more-fundamental theory. Several attempts have been made to extend the gauge symmetry of the SM via one or more U(1) gauge symmetries beyond the hypercharge gauge symmetry, $\mathrm{U}(1)_Y$ [1–12]. The evidence for non-vanishing neutrino masses, based on the apparent observation of neutrino oscillation, strongly encourages this type of extensions. In this class of models [1–8], three SM singlet fermions arise quite naturally due to the anomaly cancellation conditions. These three particles are accounted for by right handed neutrinos, and hence a natural explanation for the seesaw mechanism is obtained.

A low scale $B-L$ symmetry breaking, based on the gauge group $G_{B-L} \equiv \mathrm{SU}(3)_C \times \mathrm{SU}(2)_\mathrm{L} \times \mathrm{U}(1)_Y \times \mathrm{U}(1)_{B-L}$, has been considered recently [8]. It was shown that this model can account for the current experimental results of the light neutrino masses and their large mixing. Therefore, it can be considered as one of the strong candidates for minimal extensions of the SM. In addition, one extra neutral gauge boson corresponding to $B-L$ gauge symmetry and an extra SM singlet scalar (extra Higgs boson) are predicted. In fact, the SM Higgs sector can be generally extended by adding extra singlet scalars without enlarging its gauge symmetry group [9, 10, 13, 14]. In [8], it has been emphasized that these new particles may have a significant impact on the SM phenomenology, and hence lead to interesting signatures at large hadron collider (LHC).

The aim of this paper is to provide a comprehensive analysis for the phenomenology of such a TeV scale extension of the SM, and its potential discovery at the LHC energies. The production cross sections and the decay branching ratios of the SM-like Higgs, H, and the extra Higgs boson H' are analyzed. We also consider the decay branching ratios of the extra gauge boson, Z'.

We show that the cross sections of the Higgs production are reduced by $\sim 20\%$–30% in the interesting mass range of ~ 120–$250\,\mathrm{GeV}$ relative to the SM predictions. However, its decay branching ratios remain intact. In addition, we find that the extra Higgs boson ($\sim$ TeV) is accessible at LHC, although it has relatively small cross sections. We also examine the availability of the decay channel $H' \to HH$, which happens to have a very small partial decay width. Concerning the Z' gauge boson, the branching ratios of $Z' \to l^+l^-$ are found to be of order $\sim 20\%$ to be compared to $\sim 3\%$ of the SM $\mathrm{BR}(Z \to l^+l^-)$.

This paper is organized as follows. In Sect. 2 we review the Higgs mechanism and symmetry breaking within the minimal $B-L$ extension of the SM. We also discuss the mixing between the SM-like Higgs and the extra Higgs boson. Section 3 is devoted to the phenomenology of the two Higgs particles. The production cross sections and decay branching ratios of these Higgs particles at LHC energies are presented. In Sect. 4 we study the decay of the extra gauge boson Z'. In Sect. 5 we briefly discuss the *very light Higgs* scenario. Finally we give our concluding remarks in Sect. 6.

[a] e-mail: skhalil@itcp.it

2 $B-L$ extension of the SM

2.1 Symmetry breaking

The fermionic and kinetic sectors of the Lagrangian in the case of the $B-L$ extension are given by

$$\mathcal{L}_{B-L} = \mathrm{i}\bar{l}D_\mu\gamma^\mu l + \mathrm{i}\bar{e}_\mathrm{R}D_\mu\gamma^\mu e_\mathrm{R} + \mathrm{i}\bar{\nu}_\mathrm{R}D_\mu\gamma^\mu\nu_\mathrm{R} - \frac{1}{4}W_{\mu\nu}W^{\mu\nu} - \frac{1}{4}B_{\mu\nu}B^{\mu\nu} - \frac{1}{4}C_{\mu\nu}C^{\mu\nu}\,. \quad (1)$$

The covariant derivative D_μ is different from the SM one by the term $\mathrm{i}g''Y_{B-L}C_\mu$, where g'' is the $\mathrm{U}(1)_{B-L}$ gauge coupling constant, Y_{B-L} is the $B-L$ charge, and $C_{\mu\nu} = \partial_\mu C_\nu - \partial_\nu C_\mu$ is the field strength of $\mathrm{U}(1)_{B-L}$. The Y_{B-L} for fermions and Higgs bosons are given in Table 1.

The Higgs and Yukawa sectors of the Lagrangian are given by

$$\mathcal{L}_{B-L} = (D^\mu\phi)(D_\mu\phi) + (D^\mu\chi)(D_\mu\chi) - V(\phi,\chi) - \left(\lambda_e\bar{l}\phi e_\mathrm{R} + \lambda_\nu\bar{l}\tilde{\phi}\nu_\mathrm{R} + \frac{1}{2}\lambda_{\nu_\mathrm{R}}\bar{\nu^c}_\mathrm{R}\chi\nu_\mathrm{R} + \mathrm{h.c.}\right)\,. \quad (2)$$

Here, λ_e, λ_ν and λ_{ν_R} refer to 3×3 Yukawa matrices. The interaction terms $\lambda_\nu l\tilde{\phi}\nu_\mathrm{R}$ and $\lambda_{\nu_\mathrm{R}}\bar{\nu^c}_\mathrm{R}\chi\nu_\mathrm{R}$ give rise to a Dirac neutrino mass term $m_\mathrm{D}\simeq\lambda_\nu v$, and a Majorana mass term, $M_\mathrm{R}=\lambda_{\nu_\mathrm{R}}v'$, respectively. The $\mathrm{U}(1)_{B-L}$ and $\mathrm{SU}(2)_\mathrm{L}\times\mathrm{U}(1)_Y$ gauge symmetries can be spontaneously broken by a SM singlet complex scalar field χ and a complex SU(2) doublet of scalar fields ϕ, respectively. We consider the most general Higgs potential invariant under these symmetries, which is given by

$$V(\phi,\chi) = m_1^2\phi^\dagger\phi + m_2^2\chi^\dagger\chi + \lambda_1(\phi^\dagger\phi)^2 + \lambda_2(\chi^\dagger\chi)^2 + \lambda_3(\chi^\dagger\chi)(\phi^\dagger\phi)\,, \quad (3)$$

where $\lambda_3 > -2\sqrt{\lambda_1\lambda_2}$ and $\lambda_1,\lambda_2\geq0$, so that the potential is bounded from below. For non-vanishing vacuum expectation values (VEVs), we require $\lambda_3^2<4\lambda_1\lambda_2$, $m_1^2<0$ and $m_2^2<0$. The VEVs, $|\langle\phi\rangle| = v/\sqrt{2}$ and $|\langle\chi\rangle| = v'/\sqrt{2}$, are then given by

$$v^2 = \frac{4\lambda_2m_1^2 - 2\lambda_3m_2^2}{\lambda_3^2-4\lambda_1\lambda_2}\,,\quad v'^2 = \frac{-2(m_1^2+\lambda_1v^2)}{\lambda_3}\,.$$

Depending on the value of the λ_3 coupling, one can have $v'\gg v$ or $v'\approx v$. Therefore, the symmetry breaking scales, v and v', can be responsible for two different symmetry breaking scenarios. In our analysis we take $v=246\,\mathrm{GeV}$ and constrain the other scale, v', by the lower bounds imposed on the mass of the extra neutral gauge boson.

Table 1. $B-L$ quantum numbers for fermions and Higgs particles

particle	l	e_R	ν_R	q	ϕ	χ
Y_{B-L}	-1	-1	-1	$1/3$	0	2

After the $B-L$ gauge symmetry breaking, the gauge field C_μ (which will be called Z' in the rest of the paper) acquires the following mass:

$$m_{Z'}^2 = 4g''v'^2\,. \quad (4)$$

The experimental search for Z' at the CDF experiment leads to $m_{Z'}\gtrsim O(6\,00)\,\mathrm{GeV}$. However, the strongest limit comes from LEP II [15]:

$$m_{Z'}/g'' > 6\,\mathrm{TeV}\,. \quad (5)$$

This implies that $v'\gtrsim O(\mathrm{TeV})$. Moreover, if the coupling g'' is $<O(1)$, one can still obtain $m_{Z'}\gtrsim O(6\,00)\,\mathrm{GeV}$.

2.2 Higgs sector

In addition to the SM complex $\mathrm{SU}(2)_\mathrm{L}$ doublet, another complex scalar singlet arises in this class of models. Out of these six scalar degrees of freedom, only two physical degrees of freedom, (ϕ,χ), remain after the $B-L$ and electroweak symmetries are broken. The other four degrees of freedom are eaten by the Z', Z and $W^\pm$ bosons.

The mixing between the two Higgs scalar fields is controlled by the coupling λ_3. In fact, one finds that for positive λ_3 , the $B-L$ symmetry breaking scale, v', becomes much higher than the electroweak symmetry breaking scale, v. In this case, the SM singlet Higgs, ϕ, and the SM-like Higgs boson, χ, are decoupled and their masses are given by

$$M_\phi = \sqrt{2\lambda_1}v\,,\quad M_\chi = \sqrt{2\lambda_2}v'\,. \quad (6)$$

For negative λ_3, however, the $B-L$ breaking scale is at the same order as the electroweak breaking scale. In this scenario, a significant mixing between the two Higgs scalars exists and can affect the SM phenomenology. This mixing can be represented by the following mass matrix for ϕ and χ:

$$\frac{1}{2}M^2(\phi,\chi) = \begin{pmatrix}\lambda_1v^2 & \frac{\lambda_3}{2}vv'\\ \frac{\lambda_3}{2}vv' & \lambda_2v'^2\end{pmatrix}\,. \quad (7)$$

Therefore, the mass eigenstates fields H and H' are given by

$$\begin{pmatrix}H\\H'\end{pmatrix} = \begin{pmatrix}\cos\theta & -\sin\theta\\ \sin\theta & \cos\theta\end{pmatrix}\begin{pmatrix}\phi\\\chi\end{pmatrix}\,, \quad (8)$$

where the mixing angle θ is defined by

$$\tan2\theta = \frac{|\lambda_3|vv'}{\lambda_1v^2-\lambda_2v'^2}\,. \quad (9)$$

The masses of H and H' are given by

$$m_{H,H'}^2 = \lambda_1v^2+\lambda_2v'^2 \mp \sqrt{(\lambda_1v^2-\lambda_2v'^2)^2+\lambda_3^2v^2v'^2}\,. \quad (10)$$

We call H and H' the light and heavy Higgs bosons, respectively. In our analysis we consider a maximum mixing

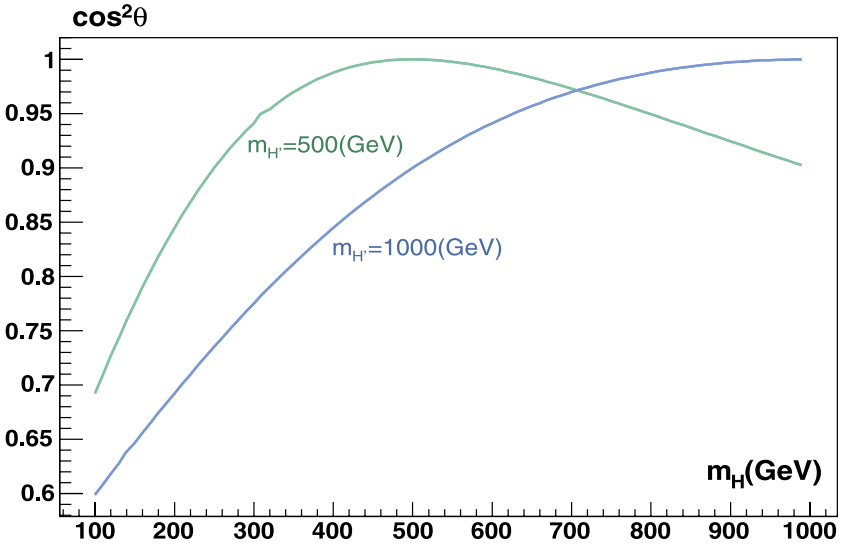

Fig. 1. H–H' mixing angle as a function of m_H for $m'_H = 500\,\text{GeV}$ and 1 TeV

between the two Higgs bosons by taking $|\lambda_3| \simeq \lambda_1^{\max}\lambda_2^{\max}$, where $\lambda_1^{\max}$ and $\lambda_2^{\max}$ are given by

$$\lambda_1^{\max} = \frac{m_H^2 + m_{H'}^2 - \sqrt{4m_H^2 m_{H'}^2 + 1} + 1}{4v^2}\,,$$
$$\lambda_2^{\max} = \frac{m_H^2 + m_{H'}^2 + \sqrt{4m_H^2 m_{H'}^2 + 1} - 1}{4v'^2}\,, \qquad (11)$$

and the maximum mixing angle is then given by

$$\tan 2\theta = \frac{\lambda_1^{\max}\lambda_2^{\max} v v'}{\lambda_1^{\max} v^2 - \lambda_2^{\max} v'^2}\,. \qquad (12)$$

By considering the maximum mixing and fixing $v = 246\,\text{GeV}$ and $v' = 1\,\text{TeV}$, we have reduced the number of free parameters of this model to just two, namely m_H and $m_{H'}$. In Fig. 1, we present the maximum mixing as a function of the light Higgs mass, m_H for $m_{H'} = 500\,\text{GeV}$ and 1 TeV.

Due to the mixing between the two Higgs bosons, the usual couplings among the SM-like Higgs, H, and the SM fermions and gauge bosons are modified. In addition, there are new couplings among the extra Higgs, H', and the SM particles:

$$g_{Hff} = \mathrm{i}\tfrac{m_f}{v}\cos\theta\,, \qquad g_{H'ff} = \mathrm{i}\tfrac{m_f}{v}\sin\theta\,,$$
$$g_{HVV} = -2\mathrm{i}\tfrac{m_V^2}{v}\cos\theta\,, \qquad g_{H'VV} = -2\mathrm{i}\tfrac{m_V^2}{v}\sin\theta\,,$$
$$g_{HZ'Z'} = 2\mathrm{i}\tfrac{m_C^2}{v'}\sin\theta\,, \qquad g_{H'Z'Z'} = -2\mathrm{i}\tfrac{m_C^2}{v'}\cos\theta\,,$$
$$g_{H\nu_R\nu_R} = -\mathrm{i}\tfrac{m_{\nu_R}}{v'}\sin\theta\,, \qquad g_{H'\nu_R\nu_R} = \mathrm{i}\tfrac{m_{\nu_R}}{v'}\cos\theta\,. \qquad (13)$$

The Higgs self-couplings are given by

$$g_{H^3} = 6\mathrm{i}\left(\lambda_1 v\cos^3\theta - \frac{\lambda_3}{2}v'\cos^2\theta\sin\theta\right)\,,$$
$$g_{H'^3} = 6\mathrm{i}\left(\lambda_2 v'\cos^3\theta + \frac{\lambda_3}{2}v\cos^2\theta\sin\theta\right)\,,$$
$$g_{H^4} = 6\mathrm{i}\lambda_1\cos^4\theta\,,$$
$$g_{H'^4} = 6\mathrm{i}\lambda_2\cos^4\theta\,,$$
$$g_{HH'^2} = 2\mathrm{i}\left(\frac{\lambda_3}{2}v\cos^3\theta + \lambda_3 v'\cos^2\theta\sin\theta - 3\lambda_2 v'\cos^2\theta\sin\theta\right)\,,$$
$$g_{H^2H'} = 2\mathrm{i}\left(\frac{\lambda_3}{2}v'\cos^3\theta - \lambda_3 v\cos^2\theta\sin\theta + 3\lambda_1 v\cos^2\theta\sin\theta\right)\,,$$
$$g_{H^2H'^2} = \mathrm{i}\lambda_3\cos^4\theta\,. \qquad (14)$$

These new couplings lead to a Higgs phenomenology different from the well known one, predicted by the SM. The detailed analysis of Higgs bosons in this class of models and their phenomenological implications, like their productions and decays at the LHC energies, will be discussed in the next section.

3 Higgs production and decay at hadron colliders

3.1 Higgs production

At the LHC, two 7-TeV proton beams with a center-of-mass energy of 14 TeV and a luminosity of $10^{34}\,\text{cm}^{-2}\text{s}^{-1}$ will collide with each other. The machine is expected to start running early 2008. The detection of the SM Higgs boson is the primary goal of the LHC project.

At hadron colliders, the two Higgs bosons couple mainly to the heavy particles: the massive gauge bosons Z', Z and $W^{\pm}$ and the heavy quarks t and b. The main production mechanisms for Higgs particles can be classified into four groups [16]: the gluon–gluon fusion mechanism [17], the associated Higgs production with heavy top or bottom quarks [18–20], the associated production with $W/Z/Z'$ bosons [21–24], and the weak vector boson fusion

processes [25–28]

$$gg \to H\,, \tag{15}$$
$$gg, q\bar{q} \to Q\bar{Q} + H\,, \tag{16}$$
$$q\bar{q} \to V + H\,, \tag{17}$$
$$qq \to V^*V^* \to qq + H\,. \tag{18}$$

The Feynman diagrams of these processes are displayed in Fig. 2. The cross sections of the Higgs production in these four mechanisms are directly proportional to the Higgs couplings with the associated particles.

In case of the gluon–gluon fusion mechanism the Higgs production is mediated by triangular loops of heavy quarks. Thus, the cross section of this process is proportional to the Higgs coupling with the heavy quark mass. In case of the $B-L$ extension of the SM, the production cross sections for the light Higgs, H, and the heavy Higgs, H', can be approximated as

$$\sigma_H \propto \alpha_s^2 \left(\frac{m_Q^2}{v^2}\cos^2\theta\right) \times |\eta(\varepsilon)|^2 \times (gg \text{ luminosity})\,, \tag{19}$$

$$\sigma_{H'} \propto \alpha_s^2 \left(\frac{m_Q^2}{v^2}\sin^2\theta\right) \times |\eta(\varepsilon')|^2 \times (gg \text{ luminosity})\,, \tag{20}$$

where the first bracket is due to the $QQH(H')$ coupling. Here, $\varepsilon = \left(4m_Q^2\right) / \left(m_H^2\right)$, $\varepsilon' = \left(4m_Q^2\right) / \left(m_{H'}^2\right)$, and

$$\eta(\varepsilon) = \frac{\varepsilon}{2}[1 + (\varepsilon - 1)\phi(\varepsilon)]\,, \tag{21}$$

with

$$\phi(\varepsilon) = \begin{cases} -\arcsin^2(1/\sqrt{2})\,, & \varepsilon \le 1\,, \\ \frac{1}{4}\left[\log\frac{1+\sqrt{1-\varepsilon}}{1-\sqrt{1-\varepsilon}} + \mathrm{i}\pi\right]^2\,, & \varepsilon > 1\,. \end{cases} \tag{22}$$

As can be seen from (19) and (20), the cross section of the light Higgs production is reduced with respect to the SM one by the factor of $\cos^2\theta$. On the other hand, the heavy Higgs production is suppressed by two factors: the small $\sin\theta$, and the large $m_{H'}$. Therefore, the heavy Higgs production is typically less than that of the light Higgs by two orders of magnitudes, i.e.,

$$\frac{\sigma_{H'}}{\sigma_H} \simeq \frac{\sin\theta^2}{\cos\theta^2}\frac{m_H^2}{m_{H'}^2} \simeq \mathcal{O}(10^{-2})\,. \tag{23}$$

Now, we consider the mechanism of Higgs production in association with heavy quark pairs, (16). In addition to the Feynman diagram shown in Fig. 2, a set of other diagrams that also contribute to this process is given in Fig. 3. Note that although this process shares its coupling with the gluon–gluon fusion process, the leading order expression of its cross section indicates that it is less by one order of magnitude, for $m_{H(H')} < 1\,\text{TeV}$. Furthermore, the ratio of $\sigma(gg \to H'Q\bar{Q})$ to $\sigma(gg \to HQ\bar{Q})$ is of order $(\sin\theta/\cos\theta)^2 \simeq \mathcal{O}(0.1)$ for $m_H < 300\,\text{GeV}$.

Finally, we study the Higgs production in association with $W/Z/Z'$ bosons and in the weak vector boson fusion processes, (17) and (18) respectively. In the $B-L$ extension of the SM, the cross sections of $q\bar{q} \to V + H$ are proportional to the mass of the gauge boson and the mixing angle θ of the two Higgs bosons,

$$V \equiv W/Z:\ \sigma_H \propto \frac{m_V^4}{v^2}\cos^2\theta \times \frac{g^2}{m_V^2} \times F(m_V^2, m_H^2, s)\,, \tag{24}$$

$$\sigma_{H'} \propto \frac{m_V^4}{v^2}\sin^2\theta \times \frac{g^2}{m_V^2} \times F(m_V^2, m_{H'}^2, s)\,, \tag{25}$$

where $F\left(m_V^2, m_H^2, s\right)$ is the usual two-body phase space function.

In case of $V \equiv Z'$, the production is enhanced by the $HZ'Z'$ coupling arising with $m_{Z'}$. However, it is suppressed by a large value of v' and the mass of the virtual gauge boson(s), $m_{Z'}$,

$$V \equiv Z':\ \sigma_H \propto \frac{m_{Z'}^4}{v'^2}\sin^2\theta \times \frac{(g''Y_{B-L}^Q)^2}{m_{Z'}^2} \times F(m_{Z'}^2, m_H^2, s)\,, \tag{26}$$

$$\sigma_{H'} \propto \frac{m_{Z'}^4}{v'^2}\cos^2\theta \times \frac{(g''Y_{B-L}^Q)^2}{m_{Z'}^2} \times F(m_{Z'}^2, m_{H'}^2, s)\,. \tag{27}$$

From these equations, one can observe that the relative ratio between the light Higgs production associated with the W/Z and Z' gauge bosons is given by $\sigma_H(W/Z)/\sigma_H(Z') \sim \cos^2\theta/\sin^2\theta \times g''^2/g^2(g'^2)$. Therefore, $\sigma_H(W/Z)$ can be larger than $\sigma_H(Z')$ by one order

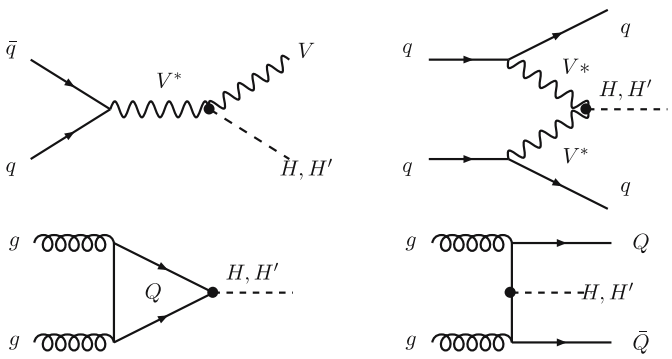

Fig. 2. The dominant Higgs boson production mechanisms in hadronic collisions

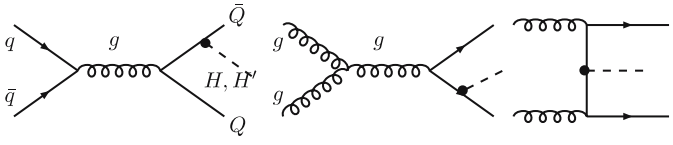

Fig. 3. Feynman diagrams for Higgs production in association with heavy quarks in hadronic collisions, $pp \to q\bar{q}, gg \to Q\bar{Q}H$, at LO

of magnitude at most. On the contrary, the situation is reversed for the heavy Higgs production and one finds that $\sigma'_H(Z') > \sigma'_H(W/Z)$, which confirms our earlier discussion. The weak vector boson fusion process, on the other hand, is relatively suppressed due to the extra Vff coupling.

The processes discussed above involve strongly interacting particles. Therefore, the lowest-order (LO) cross sections are affected by large uncertainties arising from higher-order QCD corrections. Hence, the next-to-leading order (NLO) QCD corrections to these processes should be included so that the total cross sections can be defined properly. These NLO QCD corrections consist mainly of virtual corrections with gluon exchange in the $q\bar{q}$ vertex and quark self-energy corrections [29–33]. Thus, the new couplings associated with the $B-L$ do not affect the higher-order QCD corrections. In other words, the higher-order QCD corrections in the case of $B-L$ are exactly those of the SM ones.

The cross sections for the Higgs bosons production in these channels (see (15)–(18)) have been calculated using the NLO FORTRAN codes: HIGLU, HQQ, V2HV, and VV2HV, respectively [34]. Extra subroutines have been added to these programs for the new couplings associated with the two Higgs scalars and the extra gauge boson [34]. As inputs, we use $v = 246\,\text{GeV}$, $v' = 1\,\text{TeV}$, and the center-of-mass energy $\sqrt{s} = 14\,\text{TeV}$. We also fix the mass of the extra gauge boson at $m_{Z'} = 600\,\text{GeV}$. The cross sections for the light Higgs boson production are summarized in Fig. 4 as functions of the light Higgs mass with $m_{H'} = 1\,\text{TeV}$. Figure 5, on the other hand, represents the heavy Higgs productions as functions of $m_{H'}$ with $m_H = 200\,\text{GeV}$.

As shown in Fig. 4, the salient feature of this low scale $B-L$ extension is that all cross sections of the light Higgs production are reduced by about 25%–35% in the interesting mass range: $m_H < 250\,\text{GeV}$. As in the SM, the main contribution to the production cross section comes from the gluon–gluon fusion mechanism with a few tens of pb.

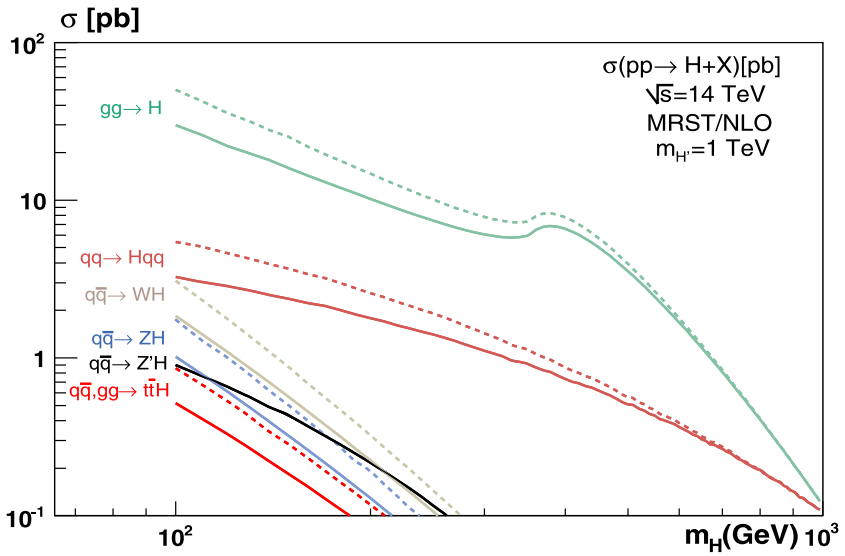

Fig. 4. The cross sections of the light Higgs production as functions of m_H: $100\,\text{GeV} \leq m_H \leq 1\,\text{TeV}$, for $m_{H'} = 1\,\text{TeV}$ and $m_{Z'} = 600\,\text{GeV}$. The solid lines indicate the reduced slope for the minimal $B-L$ extension of the SM

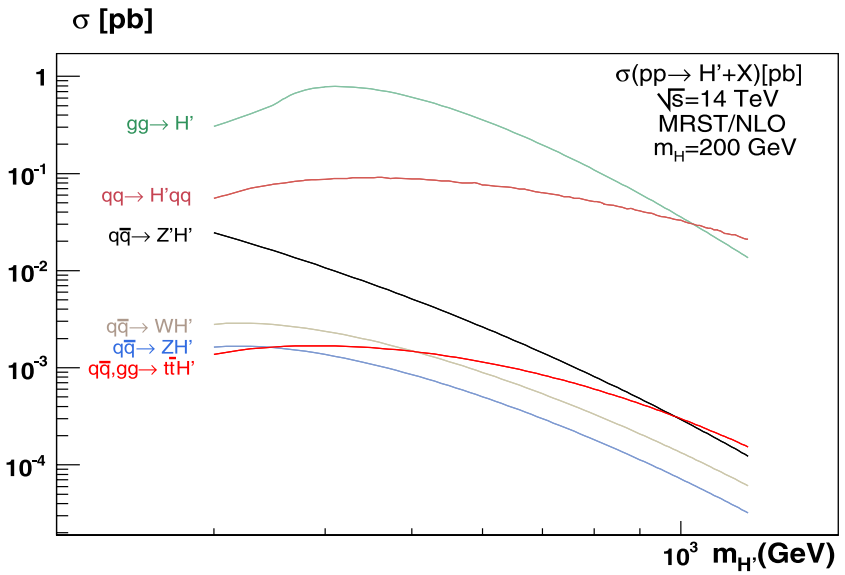

Fig. 5. The cross sections of the heavy Higgs production as functions of $m_{H'}$: $300\,\text{GeV} \leq m_{H'} \leq 1\,\text{TeV}$, for $m_H = 200\,\text{GeV}$ and $m_{Z'} = 600\,\text{GeV}$

The next relevant contribution is given by the Higgs production in the weak vector boson mechanism, (18). This contribution is at the level of a few pb, as estimated above. Furthermore, the production associated with Z/W is dominant over the production associated with Z' for $m_H < 300\,\text{GeV}$.

Now, we analyze the production of the heavy Higgs boson. It turns out that its cross sections are smaller than the light Higgs boson ones. As shown in Fig. 5, all these cross sections are scaled down by a factor $\mathcal{O}(10^{-2})$, which is consistent with the result obtained in (23). Unlike the light Higgs scenario, the production associated with Z' is dominant over the production associated with Z/W, in agreement with our previous prediction.

3.2 Higgs decay

The Higgs particle tends to decay into the heaviest gauge bosons and fermions allowed by the phase space. The Higgs decay modes can be classified into three categories: Higgs decays into fermions (Fig. 6), Higgs decays into massive gauge bosons (Fig. 7), and Higgs decays into massless gauge bosons (Fig. 8).

The decay widths into fermions are directly proportional to the Hff couplings:

$$\Gamma(H \longrightarrow ff) \approx m_H \left(\frac{m_f}{v}\right)^2 \left(1-\frac{4m_f^2}{m_H^2}\right)^{3/2} \cos^2\theta\,, \tag{28}$$

$$\Gamma(H' \longrightarrow ff) \approx m_{H'} \left(\frac{m_f}{v}\right)^2 \left(1-\frac{4m_f^2}{m_{H'}^2}\right)^{3/2} \sin^2\theta\,. \tag{29}$$

In the case of the top quark, three-body decays into on-shell and off-shell states (Fig. 9) were taken into consideration.

On the other hand, the decay widths into massive gauge bosons $V = Z', Z, W$ are directly proportional to the HVV couplings. The partial width for H and H' bosons decaying into two real gauge bosons are given by

$$\begin{aligned} V \equiv W/Z : \Gamma_H &\approx \frac{m_H^3}{v^2} f(m_V^2/m_H^2)\cos^2\theta\,, \\ \Gamma_{H'} &\approx \frac{m_{H'}^3}{v^2} f(m_V^2/m_{H'}^2)\sin^2\theta\,, \end{aligned} \tag{30}$$

$$\begin{aligned} V \equiv Z' : \Gamma_H &\approx \frac{m_H^3}{v'^2} f(m_V^2/m_H^2)\sin^2\theta\,, \\ \Gamma_{H'} &\approx \frac{m_{H'}^3}{v'^2} f(m_V^2/m_{H'}^2)\cos^2\theta\,, \end{aligned} \tag{31}$$

with

$$f(x) = \sqrt{1-4x}(1-4x+12x^2)\,. \tag{32}$$

Three-body and four-body decays were also taken into consideration in our analysis.

As shown in Fig. 8, the massless gauge bosons are not directly coupled to the Higgs bosons, but they are coupled via W, charged fermions, and quark loops. This implies that the decay widths are in turn proportional to the HVV and Hff couplings; hence they are relatively suppressed.

From the above equations, one finds that all decay widths of the light Higgs boson are proportional to $\cos^2\theta$, except the new decay mode of $Z'Z'$. Furthermore, this channel has a very small contribution to the total decay width. Therefore, the light Higgs boson branching ratios (the ratios between the partial decay widths and the total decay width) have a small dependence on the mixing parameter θ. Thus, it is expected that one will see no significant difference between the results of the light Higgs branching ratios in this model of $B-L$ extension and the SM ones. On the other hand, the heavy Higgs branching ratios have a relevant dependence on θ.

The decay widths and branching ratios of the Higgs bosons in these channels have been calculated using the FORTRAN code: HDECAY with extra subroutines for the new couplings associated with the two Higgs scalars and

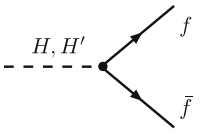

Fig. 6. The Feynman diagram for the Higgs boson decays into fermions

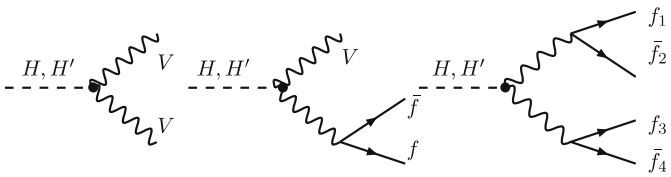

Fig. 7. Diagrams for the Higgs boson decays into massive gauge bosons

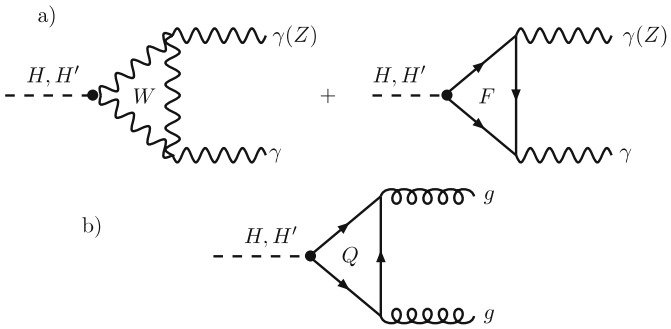

Fig. 8. Loop induced Higgs boson decays into (**a**) two photons ($Z\gamma$) and (**b**) two gluons

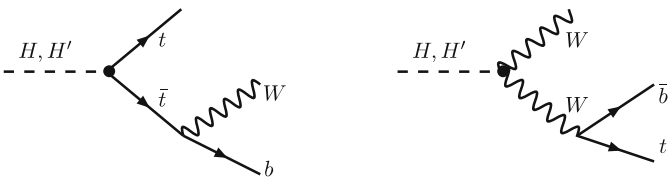

Fig. 9. Diagrams for the three-body decays of the Higgs boson into the tbW final states

the extra gauge boson [34, 35]. As in the Higgs production analysis, we use the following inputs: $v = 246\,\text{GeV}$, $v' = 1\,\text{TeV}$, $m_{Z'} = 600\,\text{GeV}$, and the c.m. energy $\sqrt{s} = 14\,\text{TeV}$. All relevant EW corrections to decays into fermions and massive gauge bosons as well as the two-loop QCD corrections to the decays into quark pairs and to the quark loop mediated decays into massless gauge bosons are taken into consideration. However, these corrections are not different from the SM ones as explained above.

The decay branching ratios of the light and heavy Higgs bosons are shown in Figs. 10 and 11, respectively, as functions of the Higgs masses. As expected, the branching ratios of the light Higgs are indistinguishable from the SM ones. In the "low mass" range, $100\,\text{GeV} < M_H < 130\,\text{GeV}$, the main decay mode is $H \to b\bar{b}$ with a branching ratio of $\sim 75\%$–50%. The decays into $\tau^+\tau^-$ and $c\bar{c}$ pairs come next with branching ratios of order $\sim 7\%$–5% and $\sim 3\%$–2%, respectively. The $\gamma\gamma$ and $Z\gamma$ decays are rare, with very small branching ratios. In the "high mass" range, $m_H > 130\,\text{GeV}$, the WW, ZZ, and to some extent the $t\bar{t}$ decays give the dominant contributions. The $Z'Z'$ decay arises for small Higgs mass (350 GeV) with a small branching ratio $\lesssim 1\%$ due to the three-body and four-body decays.

Regarding the heavy Higgs decay branching ratio, one finds that $H' \to WW$ and ZZ are the dominant decay modes, with a branching ratio of $\sim 70\%$ and $\sim 20\%$, respectively. To a lower extent, the $t\bar{t}$ and $Z'Z'$ account for the remaining branching ratios. Note that these two decay modes are in particular sensitive to the running mixing angles. Thus, they have the behaviors shown in Fig. 11. The other modes give very tiny contributions and hence they are not shown in this figure.

It is useful to mention that the heavy Higgs boson may decay to a pair of the lighter Higgs boson. The partial decay width of this channel, which can be expressed by

$$\Gamma(H' \longrightarrow HH) \approx \frac{1}{16\pi\sqrt{2}} \frac{g^2_{H^2H'}}{m_{H'}} \left(1 - \frac{4m^2_{H'}}{m^2_H}\right)^{1/2}, \tag{33}$$

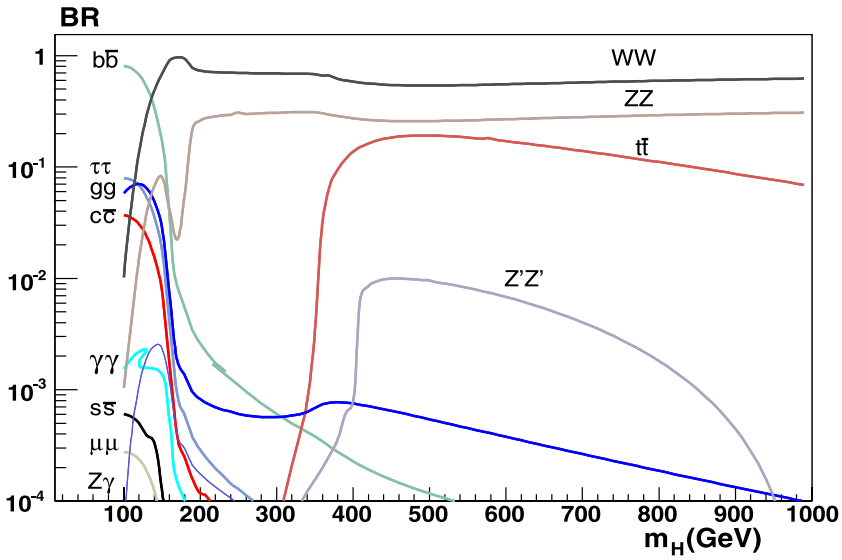

Fig. 10. The branching ratios of the light Higgs decay as functions of m_H for $m_{H'} = 1\,\text{TeV}$ and $m_{Z'} = 600\,\text{GeV}$

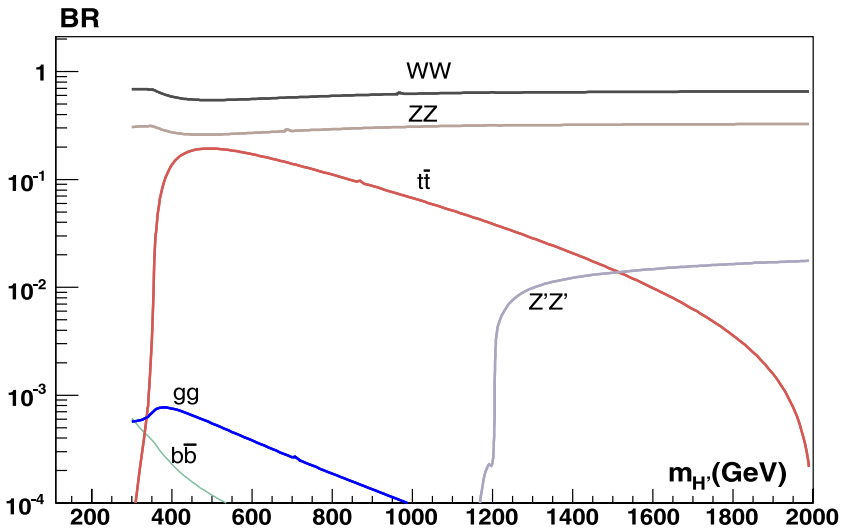

Fig. 11. The branching ratios of the heavy Higgs decay as functions of $m_{H'}$ for $m_H = 200\,\text{GeV}$ and $m_{Z'} = 600\,\text{GeV}$

is suppressed by the tiny $g_{H^2H'}$ coupling (14) and the relatively large $m_{H'}$. In fact, the resulting branching ratio of this decay mode is at the level of 10^{-8}, and hence does not appear in Fig. 11.

4 Z' decay in $B-L$ extension of the SM

In this section we study the decay of the extra gauge boson predicted by the $B-L$ extension of the SM at the LHC energies. In fact, there are many models which contain extra gauge bosons [15, 36–41]. These models can be classified into two categories depending on whether or not they arise in a GUT scenario. In some of these models, the Z' and the SM Z are not true mass eigenstates due to mixing. This mixing induces the couplings between the extra Z' boson and the SM fermions. However, there is a stringent experimental limit on the mixing parameter. In our model of $B-L$ extension of the SM, there is no tree-level Z–Z' mixing. Nevertheless, the extra $B-L$ Z' boson and the SM fermions are coupled through the non-vanishing $B-L$ quantum numbers.

The interactions of the Z' boson with the SM fermions are described by

$$\mathcal{L}_{\rm int}^{Z'} = \sum_f Y_{B-L}^f g'' Z'_\mu f \gamma^\mu f \,. \tag{34}$$

The decay widths of $Z' \to f\bar{f}$ are then given by [15]

$$\begin{aligned}
\Gamma(Z' \to l^+l^-) &\approx \frac{(g'' Y_{B-L}^l)^2}{24\pi} m_{Z'} \,, \\
\Gamma(Z' \to q\bar{q}) &\approx \frac{(g'' Y_{B-L}^q)^2}{8\pi} m_{Z'} \left(1+\frac{\alpha_{\rm s}}{\pi}\right) \,, \quad q \equiv b,c,s \,, \\
\Gamma(Z' \to t\bar{t}) &\approx \frac{(g'' Y_{B-L}^q)^2}{8\pi} m_{Z'} \left(1-\frac{m_t^2}{m_{Z'}^2}\right)\left(1-\frac{4m_t^2}{m_{Z'}^2}\right)^{1/2} \\
&\quad \times \left(1+\frac{\alpha_{\rm s}}{\pi}+O\left(\frac{\alpha_{\rm s} m_t^2}{m_{Z'}^2}\right)\right) \,.
\end{aligned} \tag{35}$$

Figure 12 shows the branching ratios of Z' decay as a function of $m_{Z'}$. Contrarily to the SM Z decay, the branching ratios of $Z' \to l^+l^-$ are relatively high compared to $Z' \to q\bar{q}$. This is due to the fact that $|Y_{B-L}^l| = 3|Y_{B-L}^q|$. Thus, one finds $\mathrm{BR}(Z' \to l^+l^-) \simeq 20\%$ to be compared to $\mathrm{BR}(Z \to l^+l^-) \simeq 3\%$. Therefore, searching for Z' can be easily accessible via a clean dilepton signal, which may be one of the first new physics signatures to be observed at the LHC.

5 Light H' scenario

In this section we discuss the possibility of having $m_{H'} \lesssim m_H$ and the phenomenological implications of this scenario. As shown in Sect. 2, the mass of the non-SM Higgs $m_{H'}$ receives a dominant contribution from the VEV of the $B-L$ symmetry breaking v' and the self-coupling λ_2. The Z' searches and the neutrino masses impose a lower limit on v': $v' \gtrsim 1\,\mathrm{TeV}$. The self-coupling λ_2 is an essentially unconstrained parameter. If $\lambda_2 \sim \mathcal{O}(1)$, then $m_{H'}$ is of order TeV as assumed in the previous sections.

There are two other interesting possibilities that have recently received some attention in the literature. The first one corresponds to the case of $\lambda_1 v^2 \sim \lambda_2 v'^2$, i.e., $\lambda_2 \sim \mathcal{O}(10^{-2})$. In this case, one finds $m_H \sim m_{H'}$, and the mixing angle is given by $\theta \sim \pi/4$. Hence, the two Higgs bosons H and H' couple similarly to the fermion and gauge fields, giving the same production cross section and decay branching ratio. Therefore, to distinguish between H and H' at LHC in this type of models is rather difficult. This scenario is usually known as *intense Higgs coupling* [42].

The second possibility concerns the case of $\lambda_2 \lesssim 10^{-3}$, in which one obtains $m_{H'} \ll m_H$. In fact, direct searches at LEP and Tevatron do not exclude a light Higgs boson with a mass below 60 GeV. Such a light Higgs boson may have escaped experimental detection due to the suppres-

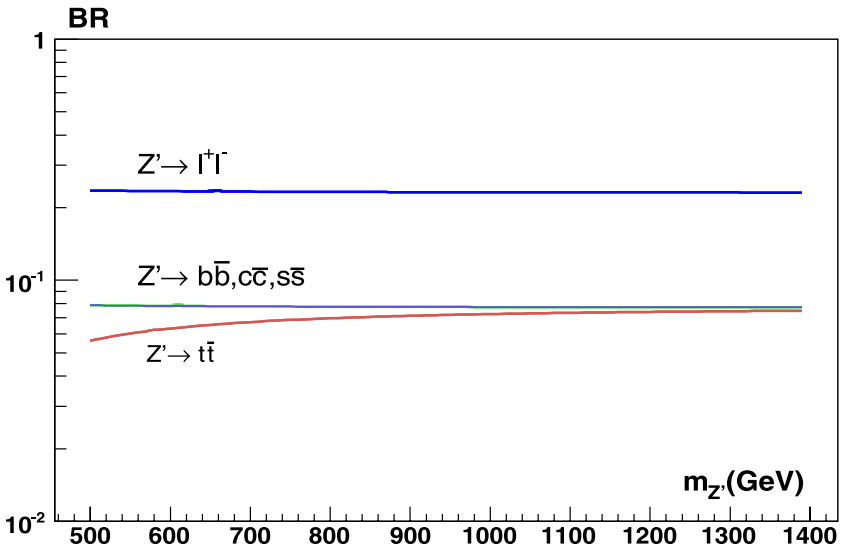

Fig. 12. The decay branching ratios of the extra gauge boson Z' as functions of $m_{Z'}$

sion of its cross sections. Therefore, a window with a very light Higgs mass still exist.

Having $\lambda_2 \lesssim 10^{-3}$ implies that λ_3 is also less than 10^{-3}. In this respect, the Higgs masses are approximately given by

$$m_H \simeq \sqrt{\lambda_1} v\,, \tag{36}$$

$$m_{H'} \simeq \mathcal{O}\left(\frac{\lambda_3 v'}{\lambda_1 v}\right) \simeq \mathcal{O}(\times 10^{-2})\ \text{GeV}\,, \tag{37}$$

and the coupling $g_{HH'H'}$ in (14) becomes very small. Thus, the decay $H \to H'H'$ is not comparable to the decay into other SM particles. The phenomenology of this scenario, derived from different SM extensions, has been studied in detail [13, 43]. In addition, this light scalar particle has been considered as an interesting candidate for dark matter [44].

6 Conclusions

In this paper we have considered the TeV scale $B-L$ extension of the SM. We provided a comprehensive analysis for the phenomenology of the SM-like Higgs, the extra Higgs scalar, and the extra gauge boson predicted in this model, with special emphasis on their discovery potential at LHC energies.

We have shown that the cross sections of the SM-like Higgs production are reduced by $\sim 20\%$–30% in the mass range of ~ 120–$250\,\text{GeV}$ compared to the SM results. On the other hand, the implications of the $B-L$ extension to the SM do not change the decay branching ratios. Moreover, we found that the extra Higgs boson has relatively small cross sections, but it is accessible at LHC energies. Finally, we showed that the branching ratios of $Z' \to l^+l^-$ are of order $\sim 20\%$, to be compared to $\sim 3\%$ of the SM $BR(Z \to l^+l^-)$. Hence, searching for Z' is accessible via a clean dilepton signal at LHC.

Acknowledgements. This work is partially supported by the ICTP under the OEA-project-30.

References

1. R.N. Mohapatra, R.E. Marshak, Phys. Rev. Lett. **44**, 1316 (1980)
2. R.E. Marshak, R.N. Mohapatra, Phys. Lett. B **91**, 222 (1980)
3. C. Wetterich, Nucl. Phys. B **187**, 343 (1981)
4. A. Masiero, J.F. Nieves, T. Yanagida, Phys. Lett. B **116**, 11 (1982)
5. R.N. Mohapatra, G. Senjanovic, Phys. Rev. D **27**, 254 (1983)
6. R.E. Marshak, R.N. Mohapatra, in: *From Su*(3) *To Gravity*, ed. by E. Gotsman, G. Tauber (Cambridge University Press, Cambridge, 2007), pp. 173–181
7. W. Buchmuller, C. Greub, P. Minkowski, Phys. Lett. B **267**, 395 (1991)
8. S. Khalil, arXiv:hep-ph/0611205
9. V. Barger, P. Langacker, G. Shaughnessy, Phys. Rev. D **75**, 055 013 (2007)
10. S. Profumo, M.J. Ramsey-Musolf, G. Shaughnessy, arXiv:hep-ph/0705.2425
11. D.G. Cerdeno, A. Dedes, T.E.J. Underwood, JHEP **0609**, 67 (2006) [arXiv:hep-ph/0607157]
12. W.F. Chang, J.N. Ng, J.M.S. Wu, arXiv:hep-ph/0701254
13. D. O'Connell, M.J. Ramsey-Musolf, M.B. Wise, Phys. Rev. D **75**, 037 701 (2007) [arXiv:hep-ph/0611014]
14. A. Datta, A. Raychaudhuri, Phys. Rev. D **57**, 2940 (1998) [arXiv:hep-ph/9708444]
15. M. Carena, A. Daleo, B.A. Dobrescu, T.M.P. Tait, Phys. Rev. D **70**, 093 009 (2004)
16. A. Djouadi, arXiv:hep-ph/0503172
17. H.M. Georgi, S.L. Glashow, M.E. Machacek, D.V. Nanopoulos, Phys. Rev. Lett. **40**, 692 (1978)
18. R. Raitio, W.W. Wada, Phys. Rev. D **19**, 941 (1979)
19. J.N. Ng, P. Zakarauskas, Phys. Rev. D **29**, 876 (1984)
20. D.A. Dicus, S. Willenbrock, Phys. Rev. D **39**, 751 (1989)
21. S.L. Glashow, D.V. Nanopoulos, A. Yildiz, Phys. Rev. D **18**, 1724 (1978)
22. J. Finjord, G. Girardi, P. Sorba, Phys. Lett. B **89**, 99 (1979)
23. E. Eichten, I. Hinchliffe, K.D. Lane, C. Quigg, Rev. Mod. Phys. **56**, 579 (1984)
24. E. Eichten, I. Hinchliffe, K.D. Lane, C. Quigg, Rev. Mod. Phys. **58**, 1065 (1986)
25. D.A. Dicus, S.S.D. Willenbrock, Phys. Rev. D **32**, 1642 (1985)
26. R.N. Cahn, S. Dawson, Phys. Lett. B **136**, 196 (1984)
27. R.N. Cahn, S. Dawson, Phys. Lett. B **138**, 464 (1984) [Erratum]
28. W. Kilian, M. Kramer, P.M. Zerwas, Phys. Lett. B **373**, 135 (1996) [arXiv:hep-ph/9512355]
29. T. Han, S. Willenbrock, Phys. Lett. B **273**, 167 (1990)
30. H. Baer, B. Bailey, J. Owens, Phys. Rev. D **47**, 2730 (1993)
31. J. Ohnemus, W. Stirling, Phys. Rev. D **47**, 2722 (1993)
32. S. Mrenna, C.P. Yuan, Phys. Lett. B **416**, 200 (1998)
33. A. Djouadi, M. Spira, Phys. Rev. D **62**, 014 004 (2000)
34. The FORTRAN codes: HIGLU, HQQ, V2HV, and VV2HV have been written by M. Spira and can be found at http://people.web.psi.ch/spira/proglist.html. The modified version was made by W. Emam and can be found at http://www.bue.edu.eg/centres/ctp/people/codes/proglist.html.
35. A. Djouadi, J. Kalinowski, M. Spira, Comput. Phys. Commun. **108**, 56 (1998) [arXiv:hep-ph/9704448]
36. J.L. Hewett, T.G. Rizzo, Phys. Rep. **183**, 139 (1989)
37. M. Cvetic, S. Godfrey, arXiv:hep-ph/9504216
38. A. Leike, Phys. Rep. **317**, 143 (1999)
39. J. Erler, P. Langacker, Phys. Lett. B **456**, 68 (1999)
40. T.G. Rizzo, arXiv:hep-ph/0610104
41. Particle Data Group, W.M. Yao et al., J. Phys. G **33**, 1 (2006)
42. E. Boos, A. Djouadi, M. Muhlleitner, A. Vologdin, Phys. Rev. D **66**, 055 004 (2002) [arXiv:hep-ph/0205160]
43. M. Krawczyk, P. Mattig, J. Zochowski, Eur. Phys. J. C **19**, 463 (2001) [arXiv:hep-ph/0009201]
44. C. Boehm, J. Orloff, P. Salati, Phys. Lett. B **641**, 247 (2006) [arXiv:astro-ph/0607437]